

Synthesis of atomically thin GaSe wrinkles for strain sensors

Cong Wang^{1,2,*}, Sheng-Xue Yang^{3,*}, Hao-Ran Zhang², Le-Na Du², Lei Wang², Feng-You Yang²,
Xin-Zheng Zhang^{1,†}, Qian Liu^{1,2,‡}

¹The MOE Key Laboratory of Weak-Light Nonlinear Photonics, TEDA Applied Physics Institute and School of Physics, Nankai University, Tianjin 300457, China

²National Center for Nanoscience and Technology, No. 11 Beiyitiao, Zhongguancun, Beijing 100190, China

³School of Materials Science and Engineering, Beihang University, Beijing 100191, PR China

Corresponding authors. E-mail: [†]zcx@nankai.edu.cn, [‡]liuq@nanoctr.cn

Received July 14, 2015; accepted September 12, 2015

A wrinkle-based thin-film device can be used to develop optoelectronic devices, photovoltaics, and strain sensors. Here, we propose a stable and ultrasensitive strain sensor based on two-dimensional (2D) semiconducting gallium selenide (GaSe) for the first time. The response of the electrical resistance to strain was demonstrated to be very sensitive for the GaSe-based strain sensor, and it reached a gauge factor of -4.3 , which is better than that of graphene-based strain sensors. The results show us that strain engineering on a nanoscale can be used not only in strain sensors but also for a wide range of applications, such as flexible field-effect transistors, stretchable electrodes, and flexible solar cells.

Keywords GaSe wrinkles, strain sensor

PACS numbers 68.65.Ac, 73.63.Bd, 71.20.Nr

1 Introduction

Since two-dimensional (2D) graphene was discovered by Geim and Novoselov in 2004, graphene has attracted increasing attention due to its excellent physical and chemical properties, such as large electron and hole mobility and unique optical, magnetic, and mechanical properties [1–7]. Graphene-based devices have been widely studied because of their significant potential use in radiofrequency, optoelectronics, battery energy, graphene plasmonics, and logic applications [8–12]. The most important advantage of graphene-based field effect transistors (FETs) is their high mobility, whereas their shortage induced by the “zero band gap” of natural graphene limited switch ratio [13]. In order to “open” the band gap of graphene, many methods such as fabrication of graphene nanoribbons and strain engineering have been used; however, only very small band gaps can be opened, which limits the wide use of graphene FETs. In order to overcome these limitations in graphene, semiconducting layered transition metal dichalcogenides (TMDs) with different bandgaps, e.g., MoS₂, WS₂, WSe₂, and GaSe, have attracted increasing interest [14–22].

As a member of the TMDs family, GaSe has attracted significant attention owing to its excellent electronic structure [23–26]. There are several kinds of GaSe with different crystal structures, such as β -GaSe, ε -GaSe, and γ -GaSe [27]. Different from semimetal graphene by the absence of a bandgap, monolayer GaSe is a p-type semiconductor with a sizable indirect band gap of 2.11 eV. Compared to graphene with a zero bandgap, this typical feature shows that GaSe can be widely used in high-performance photodetectors and FETs with high current ON/OFF ratios. Like graphene, many other layered materials, especially from the TMD family, have been obtained through the micromechanical cleavage technique, which has been applied to obtain high-quality single crystals. These single crystals are very suitable for laboratory research into a material’s physical behavior. Recently, 2D atomically thin GaSe, which can be synthesized through the micromechanical cleavage technique, vapor-phase deposition, or epitaxy growth, has shown perfect linear and nonlinear optical properties (such as a strong second harmonic generation effect), perfect FET characteristics and photodetectors, indicating the significant potential of this 2D nanomaterial in such devices [23, 27–29]. However, the use of GaSe in strain sensors has not been studied.

In this work, the structure of GaSe was analyzed. Also,

*These authors contributed equally to this work.

we propose a GaSe strain sensor with a gauge factor of -4.3 for the first time, based on the transport properties of wrinkled GaSe under different uniaxial tensile strain.

2 Experimental details

The bulk GaSe crystals were grown by using a modified Bridgman growth technique. GaSe flakes were obtained through a mechanical exfoliation technique by using Scotch tape and then transferred onto a 300 nm SiO_2/Si substrate. Then we used an optical microscope (LEICA DM2500M supplemented with an LEICA DFC425 digital camera) to choose the thickness of GaSe nanosheets according to the big differences between different thickness GaSe flakes on the 300 nm SiO_2/Si substrate.

The crystal structures of the GaSe nanosheets were analyzed by high-resolution transmission electron microscopy (HRTEM) using an FEI Tecnai G2 F20 U-TWIN at a voltage of 200 kV at low dose densities; no detectable damage was observed during imaging. The morphologies of the GaSe flakes were observed by field emission scanning electron microscopy (Hitachi S-4800) at a voltage of 10 kV. The energy dispersive X-ray spectroscopy (EDS) analysis was carried out using the same scanning electron microscopy (SEM) equipment.

As for the GaSe strain sensor device fabrication, the GaSe flakes were first deposited onto a 300 nm SiO_2/Si substrate by using Scotch tape from bulk GaSe. We then used an optical microscope to choose a suitable GaSe sample. The GaSe/ SiO_2/Si sample was baked on a hot plate at 180 °C for 5 min. A polymethyl methacrylate (PMMA) film approximately 1000 nm thick was then spin coated on the GaSe/ SiO_2/Si sample through a photoresist spinner at 3000 rpm ($50 \text{ rpm}\cdot\text{s}^{-1}$) and then baked at 180 °C for 2 min. After that, the sample was exposed by electron-beam lithography through an SEM/focused ion beam system (Nava 200 NanoLab) for electrode fabrication at a voltage of 30 kV and a current of 1.5 nA. For the electrodes, a 5-nm-thick layer of Cr followed by a 30-nm-thick layer of Au was deposited by using electron beam evaporation. Then, well-defined source and drain electrodes were achieved by using the lift-off process with acetone/IPA. Finally, the two-terminal GaSe devices were transferred from the SiO_2/Si substrate to a prestrained polydimethylsiloxane (PDMS) substrate through polymethyl methacrylate (PMMA) film as a transfer medium. Acetone was then used to remove the PMMA, and the prestrained PDMS was slowly released for fabrication of a GaSe wrinkled strain device. A semiconductor device analyzer system (4200-SCS) was used to measure the electrical properties at room temperature.

3 Results and discussion

Layered GaSe has planar tetra-layer (TL) structures with weak van der Waals forces, which allows GaSe samples to be fabricated down to 1 TL by the micromechanical cleavage technique from bulk material using adhesive tape. As a layered semiconductive material, each TL consisted of Se–Ga–Se–Ga sheets held together by relatively weak interlayer coupling. Each TL in the GaSe crystal had a thickness of approximately 0.798 nm [Fig. 1(a)] [24]. Figure 1(b) shows a typical SEM image of the 2D GaSe crystals on a SiO_2/Si substrate. The thicker regions of the layered GaSe correspond to areas of brighter contrast and thinner regions correspond to areas of darker contrast.

EDS is an analytical technique used for the elemental analysis or chemical characterization of a sample. To further confirm the detailed composition of the GaSe flakes, EDS analysis was carried out on the same sample shown in Fig. 1(b). As shown in Fig. 2, EDS measurements indicate the existence of Ga and Se elements in the GaSe nanoflakes, with an atomic ratio of approximately 1:1.

In order to study the crystal structures and their crystal quality, the 2D GaSe crystals were also characterized by TEM. The thin GaSe nanosheets were first cleaned by ultrasound in alcohol, then transferred on a Quantifoil[®] TEM grid. Figure 3(a) displays the low-magnification TEM images of the GaSe flakes. The HRTEM image in Fig. 3(b) shows a lattice spacing of

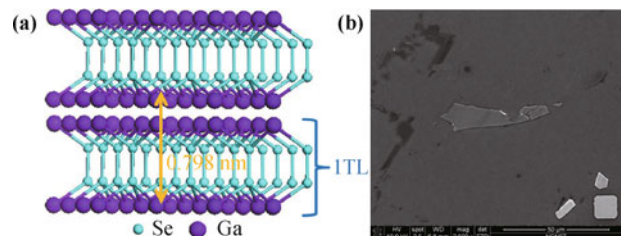


Fig. 1 (a) Layered crystal structure of GaSe with each tetra-layer (TL) formed by Se–Ga–Se–Ga atomic sheets. (b) SEM images of GaSe crystals.

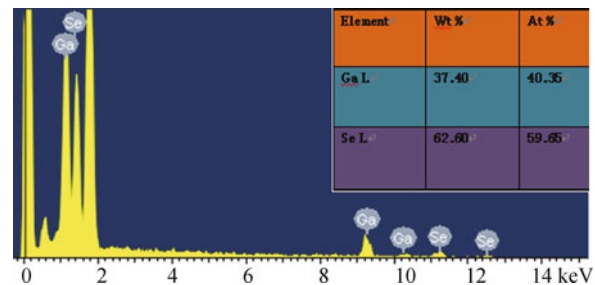


Fig. 2 The energy dispersive X-ray spectroscopy (EDS) of GaSe flakes.

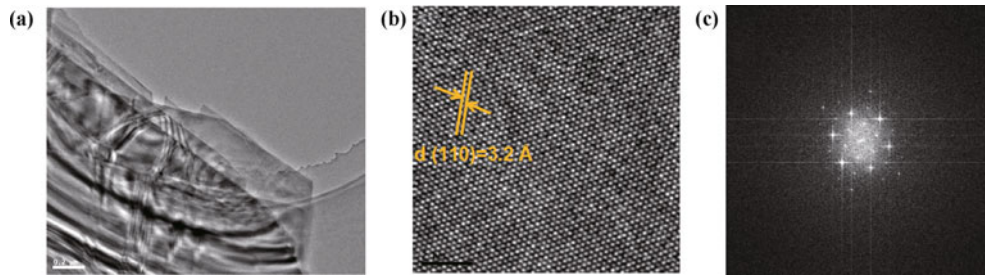


Fig. 3 (a) TEM images of few layered GaSe sheet at low magnification; (b) at high resolution; (c) The corresponding Fast Fourier Transforms (FFT).

3.2 Å in the stacked GaSe TLs, corresponding to the (110) lattice plane along the [001] zone axis. The corresponding fast Fourier transform (FFT) image [Fig. 3(c)] shows only one set of six-fold-symmetry diffraction spots, which confirms the nature single crystalline characteristics with a hexagonal crystal structure.

Strain engineering has been widely used for tuning the resistance of materials for strain sensors in various semiconductors and metals. When applying strain on atomically thin GaSe, the geometry and resistivity will change. This will make the electrical properties strongly dependent on the applied tensile strain. The high electrical-mechanical coupling behavior for GaSe films indicates potential application in high-level strain sensors for flexible electronic devices. Figure 4(a) shows the probe station used to measure the properties of the wrinkled GaSe

sensor device. Figure 4(b) shows typical current–voltage (I – V) curves of the wrinkled GaSe strain device under different tensile strains. It can be observed that the relationship between current and bias voltage is linear, indicating good ohmic contact between the GaSe film and the metal electrodes. Figure 4(c) shows the details of the linear resistance–strain characteristics. As the tensile strain increases from 0% to 20% (the wrinkled strained GaSe flattens under a 20% strain), the resistance linearly decreases from $2.7 \times 10^8 \Omega$ to $0.7 \times 10^8 \Omega$ naturally, as shown in Fig. 4(c), due to the increase in scattering of the charge carriers. The sensitivity of the electrical-mechanical coupling is defined by the gauge factor (GF) [30], which is defined as

$$GF = [R(\varepsilon)/R(0) - 1]/\varepsilon,$$

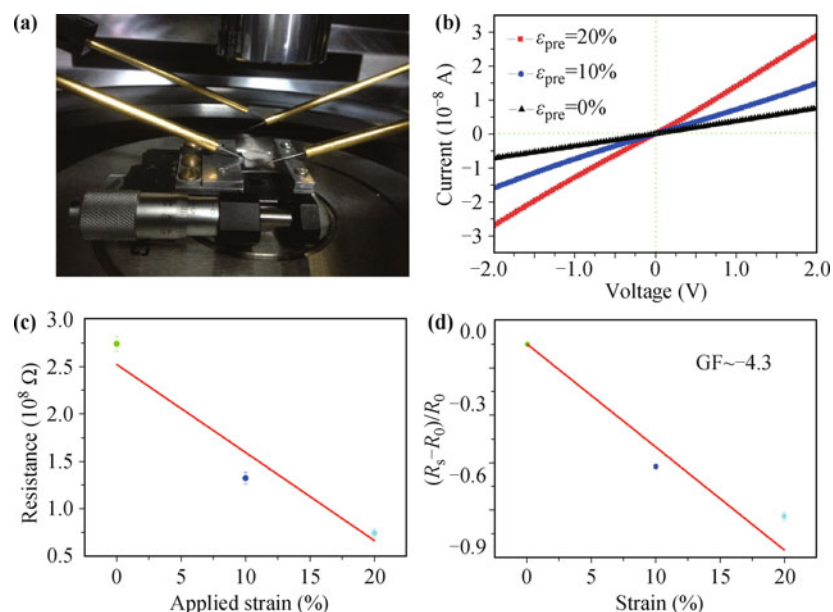


Fig. 4 Comparison of resistance response under different strain of wrinkled GaSe device. (a) Experiment setup to measure the strain effect of wrinkled GaSe sensor device. (b) I – V curves of a two-terminal GaSe wrinkles device under different pre-strains. (c) Resistance response of the wrinkled GaSe device under different strain, every Resistance at different strain is the average value at three voltages at three different voltage of -2 V, 2 V and 1 V, both experimental data and line fit are shown. (d) Resistance modulation of this wrinkled device showing a $GF \sim 4.3$, every Resistance at different strain is the average value at three voltages at three different voltage of -2 V, 2 V and 1 V, both experimental data and line fit are shown.

where $R(0)$ is the resistance of the sensor under zero strain, $R(\varepsilon)$ is the resistance under the strain, and ε is the tensile strain, which reflects the deformation of GaSe. Figure 4(d) shows the line fit and experimental data of the resistance modulation of the particular device. The GF is approximately -4.3 , which is better than that of the graphene wrinkled strain device [31].

4 Summary and conclusion

In conclusion, we fabricated few-layered GaSe and analyzed its structure. The current–voltage characteristics for the wrinkled GaSe strain device under different stretching showed a GF of -4.3 , which is better than that graphene wrinkled strain device, demonstrating the application potential of GaSe strain sensors with high performance. This study provides a new method for constructing GaSe strain sensors.

Acknowledgements This research was supported by the National Natural Science Foundation of China (Grant No. 10974037), the Chinese Academy of Sciences Strategy Pilot program (Grant No. XAD 09020300), and the National Basic Research Program of China (Grant No. 2010CB934102).

References

1. K. R. Allakhverdiev, M. O. Yetis, S. Ozbek, T. K. Baykara, and E. Y. Salaev, Effective nonlinear GaSe crystal: Optical properties and applications, *Laser Phys.* 19(5), 1092 (2009)
2. K. Novoselov, D. Jiang, F. Schedin, T. Booth, V. Khotkevich, S. Morozov, and A. Geim, Two-dimensional atomic crystals, *Proc. Natl. Acad. Sci. USA* 102(30), 10451 (2005)
3. K. Novoselov, A. K. Geim, S. Morozov, D. Jiang, M. Katsnelson, I. Grigorieva, S. Dubonos, and A. Firsov, Two-dimensional gas of massless Dirac fermions in graphene, *Nature* 438(7065), 197 (2005)
4. Y. Zhang, Y. W. Tan, H. L. Stormer, and P. Kim, Experimental observation of the quantum Hall effect and Berry's phase in graphene, *Nature* 438(7065), 201 (2005)
5. J. W. Jiang, Graphene versus MoS₂: A short review, *Front. Phys.* 10(3), 106801 (2015)
6. W.-J. Li, D. X. Yao, and E. W. Carlson, Tunable nano Peltier cooling device from geometric effects using a single graphene nanoribbon, *Front. Phys.* 9(4), 472 (2014)
7. C. Stampfer, J. Güttinger, F. Molitor, C. Volk, B. Terrés, J. Dauber, S. Engels, S. Schnez, A. Jacobsen, S. Droscher, T. Ihn, and K. Ensslin, Transport in graphene nanostructures, *Front. Phys.* 6, 271 (2011)
8. K. Novoselov, E. McCann, S. Morozov, V. I. Fal'ko, M. Katsnelson, U. Zeitler, D. Jiang, F. Schedin, and A. Geim, Unconventional quantum Hall effect and Berry's phase of 2p in bilayer graphene, *Nat. Phys.* 2(3), 177 (2006)
9. K. S. Kim, Y. Zhao, H. Jang, S. Y. Lee, J. M. Kim, K. S. Kim, J. H. Ahn, P. Kim, J. Y. Choi, and B. H. Hong, Large-scale pattern growth of graphene films for stretchable transparent electrodes, *Nature* 457(7230), 706 (2009)
10. A. K. Geim and K. S. Novoselov, The rise of graphene, *Nat. Mater.* 6(3), 183 (2007)
11. Z. Fang, Y. Wang, Z. Liu, A. Schlather, P. M. Ajayan, F. H. Koppens, P. Nordlander, and N. J. Halas, Plasmon-induced doping of graphene, *ACS Nano* 6(11), 10222 (2012)
12. Z. Fang, Y. Wang, A. E. Schlather, Z. Liu, P. M. Ajayan, F. J. García de Abajo, P. Nordlander, X. Zhu, and N. J. Halas, Active tunable absorption enhancement with graphene nanodisk arrays, *Nano Lett.* 14(1), 299 (2013)
13. J. Feng, W. Li, X. Qian, J. Qi, L. Qi, and J. Li, Patterning of graphene, *Nanoscale* 4(16), 4883 (2012)
14. B. Radisavljevic, A. Radenovic, J. Brivio, V. Giacometti, and A. Kis, Single-layer MoS₂ transistors, *Nat. Nanotechnol.* 6(3), 147 (2011)
15. A. Splendiani, L. Sun, Y. Zhang, T. Li, J. Kim, C. Y. Chim, G. Galli, and F. Wang, Emerging photoluminescence in monolayer MoS₂, *Nano Lett.* 10(4), 1271 (2010)
16. H. Zeng, J. Dai, W. Yao, D. Xiao, and X. Cui, Valley polarization in MoS₂ monolayers by optical pumping, *Nat. Nanotechnol.* 7(8), 490 (2012)
17. T. Scrace, Y. Tsai, B. Barman, L. Schweidenback, A. Petrou, G. Kioseoglou, I. Ozfidan, M. Korkusinski, and P. Hawrylak, Magnetoluminescence and valley polarized state of a two-dimensional electron gas in WS₂ monolayers, *Nat. Nanotechnol.* 10(7), 603 (2015)
18. E. J. Sie, J. W. McIver, Y. H. Lee, L. Fu, J. Kong, and N. Gedik, Valley-selective optical Stark effect in monolayer WS₂, *Nat. Mater.* 14(3), 290 (2014)
19. A. Srivastava, M. Sidler, A. V. Allain, D. S. Lembke, A. Kis, and A. Imamoglu, Valley Zeeman effect in elementary optical excitations of monolayer WSe₂, *Nat. Phys.* 11(2), 141 (2015)
20. A. M. Jones, H. Yu, J. S. Ross, P. Klement, N. J. Ghimire, J. Yan, D. G. Mandrus, W. Yao, and X. Xu, Spin-layer locking effects in optical orientation of exciton spin in bilayer WSe₂, *Nat. Phys.* 10(2), 130 (2014)
21. X. Zhou, J. Cheng, Y. Zhou, T. Cao, H. Hong, Z. Liao, S. Wu, H. Peng, K. Liu, and D. Yu, Strong second-harmonic generation in atomic layered GaSe, *J. Am. Chem. Soc.* (2015)
22. X. Yuan, L. Tang, S. Liu, P. Wang, Z. G. Chen, C. Zhang, Y. Liu, W. Wang, Y. Zou, C. Liu, N. Guo, J. Zou, P. Zhou, W. Hu, and F. Xiu, Arrayed van der Waals vertical heterostructures based on 2D GaSe grown by molecular beam epitaxy, *Nano Lett.* 15(5), 3571 (2015)
23. D. J. Late, B. Liu, J. Luo, A. Yan, H. S. Matte, M. Grayson, C. N. Rao, and V. P. Dravid, GaS and GaSe ultrathin layer transistors, *Adv. Mater.* 24(26), 3549 (2012)

24. S. Lei, L. Ge, Z. Liu, S. Najmaei, G. Shi, G. You, J. Lou, R. Vajtai, and P. M. Ajayan, Synthesis and photoresponse of large GaSe atomic layers, *Nano Lett.* 13(6), 2777 (2013)
25. Y. Zhou, Y. Nie, Y. Liu, K. Yan, J. Hong, C. Jin, Y. Zhou, J. Yin, Z. Liu, and H. Peng, Epitaxy and photoresponse of two-dimensional GaSe crystals on flexible transparent mica sheets, *ACS Nano* 8(2), 1485 (2014)
26. Y. Cao, K. Cai, P. Hu, L. Zhao, T. Yan, W. Luo, X. Zhang, X. Wu, K. Wang, and H. Zheng, Strong enhancement of photoresponsivity with shrinking the electrodes spacing in few layer GaSe photodetectors, *Sci. Rep.* 5, 8130 (2015)
27. X. Li, M. W. Lin, A. A. Puretzky, J. C. Idrobo, C. Ma, M. Chi, M. Yoon, C. M. Rouleau, and D. B. Kravchenko, Geohegan, and K. Xiao, Controlled vapor phase growth of single crystalline, two-dimensional GaSe crystals with high photoresponse, *Sci. Rep.* 4, 5497 (2014)
28. L. Karvonen, A. Säynätjoki, S. Mehravar, R. D. Rodriguez, S. Hartmann, D. R. Zahn, S. Honkanen, R. A. Norwood, N. Peyghambarian, and K. Kieu, Investigation of second- and third-harmonic generation in few-layer gallium selenide by multiphoton microscopy, *Sci. Rep.* 5, 10334 (2015)
29. W. Jie, X. Chen, D. Li, L. Xie, Y. Y. Hui, S. P. Lau, X. Cui, and J. Hao, Layer-dependent nonlinear optical properties and stability of non-centrosymmetric modification in few-layer gase sheets, *Angew. Chem.* 127(4), 1201 (2015)
30. J. Zhao, C. He, R. Yang, Z. Shi, M. Cheng, W. Yang, G. Xie, D. Wang, D. Shi, and G. Zhang, Ultra-sensitive strain sensors based on piezoresistive nanographene films, *Appl. Phys. Lett.* 101(6), 063112 (2012)
31. Y. Wang, R. Yang, Z. W. Shi, L. C. Zhang, D. X. Shi, E. Wang, and G. Y. Zhang, Super-elastic graphene ripples for flexible strain sensors, *ACS Nano* 5(5), 3645 (2011)